

Effect of organic solvents on catalyst structure of PEM fuel cell electrode fabricated via electrospray deposition

Bum-Soo Koh^a and Sung-Chul Yi^{a,b,*}

^aDepartment of Chemical Engineering, Hanyang University, Seoul 133-791, Korea

^bDepartment of Hydrogen and Fuel Cell Technology, Hanyang University, Seoul 133-791, Korea

Proton exchange membrane fuel cells (PEMFCs) are some of the most efficient electrochemical energy sources for transportation applications because of their clean, green, and high efficiency characteristics. The optimization of catalyst layer morphology is considered a feasible approach to achieve high performance of PEMFC membrane electrode assembly (MEA). In this work, we studied the effect of the solvent on the catalyst layer of PEMFC MEAs fabricated using the electrostatic spray deposition method. The catalyst ink comprised of Pt/C, a Nafion ionomer, and a solvent. Two types of solvent were used: isopropyl alcohol (IPA) and dimethylformamide (DMF). Compared with the catalyst layer prepared using IPA-based ink, the catalyst layer prepared with DMF-based ink had a dense structure because the DMF dispersed the Pt/C-Nafion agglomerates smaller and more homogeneously. The size distribution of the agglomerates in catalyst ink was confirmed through Dynamic Light Scattering (DLS) and the microstructure of the catalyst layer was compared using field emission scanning electron microscopy (FE-SEM). In addition, the electrochemical investigation was performed to evaluate the solvent effect on the fuel cell performance. The catalyst layer prepared with DMF-based ink significantly enhanced the cell performance (1.2 A cm^{-2} at 0.5 V) compared with that fabricated using IPA-based ink (0.5 A cm^{-2} at 0.5 V) due to the better dispersion and uniform agglomeration on the catalyst layer.

Key words: PEMFC, MEA, Solvent effect, Electrospray Deposition.

Introduction

Proton exchange membrane fuel cells (PEMFCs) are some of the most promising energy sources for a wide variety of power applications, including portable, stationary, and transportation applications. PEMFCs have numerous advantages such as low-operating temperatures, eco-friendliness, high-energy efficiency and high specific energy [1]. However, one of the essential problems with fuel cells is the need to reduce the platinum (Pt) content in the electrodes because of the high cost and scarcity of Pt. Therefore, improving the performance of PEMFCs with low Pt content by optimizing the catalyst layer structure is essential [2].

To address this issue, numerous researchers have extensively investigated the development of thin catalyst layers and the increase of the fuel cell performance with low Pt loading. In order to create a thin film and reduce the Pt content in the catalyst layer, various methods have been attempted. Bruno G. Pollet invented a technique for ultra-low Pt loading of a catalyst layer on a gas diffusion layer using ultrasonic spray deposition [3]. This technique was applied on a high-

temperature substrate, which is advantageous when using high boiling point solvents [4]. Despite this advantage, there are several issues: i) this method cannot adapt to polymer membrane because the membrane dissolved at a high temperature of the environment, ii) multiple manufacturing steps are required, and iii) the performance of cells prepared using the catalyst-coated membrane (CCM) method is higher than that for cells prepared using the catalyst-coated gas diffusion layer (CCG) method. Therefore, it is essential to adapt the CCM method for commercialization. There are several CCM methods such as piezo-electric printing and electro-spray deposition available for fabricating thin film catalysts on a membrane. Using a piezoelectric printer, Karan et al. fabricated a thin film catalyst layer of PEMFC MEAs with ultra-low Pt loading, which coated on the membrane directly [5]. In spite of the success in fabricating ultra-low Pt loading electrodes, this method is unsuitable for coating the large electrode areas. Among the various methods, the electro-spray deposition is capable to coat the large electrodes and thin film catalyst layer. Benitez et al. was the first established research group to use electro-spray deposition for thin film catalyst layers on PEMFC electrodes [6, 7]. By comparing the resulting catalyst layers with general-sprayed catalyst layers, they demonstrated that the electro-sprayed catalyst layer had more than double the power density at a high Pt

*Corresponding author:
Tel : +82-2-2220-0481
Fax: +82-2-2298-5147
E-mail: scyi@hanyang.ac.kr

loading of 0.5 mg cm^{-2} . In addition, Chaparro et al. investigated the optimization of the catalyst slurry composition, the dispersing solvents, and the Nafion ionomer content [8, 9]. The amount of Nafion ionomer required for the catalyst slurry was lower than that of the conventional slurry, indicating that the interaction between the Nafion ionomer and the Pt/C catalyst was remarkably improved with the electro-spray method. Later, Chaparro et al. and Martin et al. both succeeded in manufacturing high-performance membrane electrode assemblies (MEAs) with a performance of approximately 600 to 700 mW cm^{-2} , at the extremely low Pt loading of 0.02 mg cm^{-2} [10-12]. Inspired by their works, many other researchers have investigated low Pt-loaded catalyst layers deposited directly on Nafion membranes as an alternative to gas diffusion layers [13-16].

In this paper, two catalyst layers were prepared via electro-spray deposition. The starting catalyst inks contained two types of solvents: isopropyl alcohol (IPA) and dimethylformamide (DMF). Each solvent has different evaporation temperatures, dielectric constants, and degree of Nafion ionomer dispersion. In particular, we examined the size distribution of Pt/C-Nafion agglomerates in each catalyst ink using DLS analysis and identified the microstructure of each catalyst layer using FE-SEM [17]. Furthermore, the increment of performance was evaluated using cell polarization curves and the electrochemical properties were thoroughly explored with electrochemical impedance spectroscopy (EIS).

Experimental

Catalyst ink formulation

The catalyst ink was prepared by mixing a concentration of 5 wt% Nafion solution (DE521, Ion Power) and a carbon-supported platinum catalyst (HiSPEC 3000, Alfa Aesar) in the selected solvent. Two pure solvents were used to prepare the dispersing mediums: dimethylformamide (DMF) (Sigma Aldrich, anhydrous, 99.8%) and isopropyl alcohol (IPA) (DAEJUNG Chemical Co., Korea). The catalyst inks were stirred with a magnetic bar for 24 hrs at room temperature, and subsequently dispersed in a sonication bath for 2 hrs to obtain a homogenous solution. To compare the size of the agglomerates in the solvent, the size distribution was measured using Dynamic Light Scattering (DLS) (ELS-Z-1000, Photol Otsuka Electronics).

MEA preparation and characterization

Before proceeding with the experiment, the Nafion membrane had to be cleared of organic and inorganic materials. Thus, the Nafion membrane was treated as follows. First, it was treated in distilled water for 1 h, then treated in 3% H_2O_2 solution for 1 h, in distilled water for 1 h, in 1 M H_2SO_4 solution for 2 h and finally in distilled water for 1 h. All processes were performed at 80°C . Finally, the treated membrane was dried for 1

day in a convection oven at 40°C [18].

An electrostatic spray machine (NANONC, ESR200R2) was utilized for coating the pretreated Nafion membrane. The machine was composed of a high voltage generator, a syringe pump, and a conductive substrate. The syringe was filled with the prepared ink and connected to a metal nozzle with internal and external diameters of $210 \mu\text{m}$ and $410 \mu\text{m}$, respectively. During the electro-spray process, the following parameters were kept constant: flow rate of 0.4 mL/hr , electrode area of 9 cm^2 , substrate temperature of 60°C , distance between the metal nozzle and the substrate of 7 cm , and voltage applied to the metal nozzle of $7\text{--}9 \text{ kV}$. When the amount of Pt in the electrodes reached 0.05 mg cm^{-2} , the MEA was rinsed with distilled water for 1 hr and stored in a convection oven at 40°C .

To obtain microstructure images of the surface and the cross-sectional regions of the electrode, the samples were studied using field emission scanning electron microscope (FE-SEM) (JSM-5600LV, JEOL). Samples with a size of $4 \text{ mm} \times 4 \text{ mm}$ were prepared in the center of the electrode.

Electrochemical characterization

To examine cell polarization, the prepared MEAs were sandwiched in two carbon papers with microporous layers (10BC, SGL) and assembled into three serpentine cell fixtures of 9 cm^2 . High purity (99.999%) hydrogen and oxygen gases were supplied to the cell at 70°C , with ambient pressure and relative humidity (RH 100). To obtain stable performance data, the cell was activated by supplying a gas at a fixed flow rate of 100 sccm for 24 hrs before characterization [19]. During the cell activation process, the cell voltage was fixed at 0.40 V to avoid critical degradation of the MEA, which is usually observed in high potential conditions. After the activation, the single cell performance was evaluated by measuring the polarization curves using a cell station for PEMFCs (Smart 2, Wonatech). EIS images were then obtained at 0.80 V and 0.50 V using a potentiostat/galvanostat as an impedance analyzer (Gamry Reference 300, Gamry Instruments). The AC amplitude and the frequency range were set as 5 mV and $20,000 \text{ Hz}$ – 0.1 Hz , respectively.

Results and Discussion

Morphology of the films

A schematic illustration of the electro-spray process is shown in Fig. 1. Firstly, the catalyst ink passing through the metallic nozzle was broken up into small charged droplets by applying a voltage higher than 6 kV , and an electric field was simultaneously created between the nozzle and substrate. The droplets were primarily composed of Pt/C catalyst aggregates covered with the Nafion ionomer, which adsorb sufficient amounts of solvent molecules. When the spray pump was actuated, the droplets drifted toward the Nafion membrane sample leaning onto the substrate

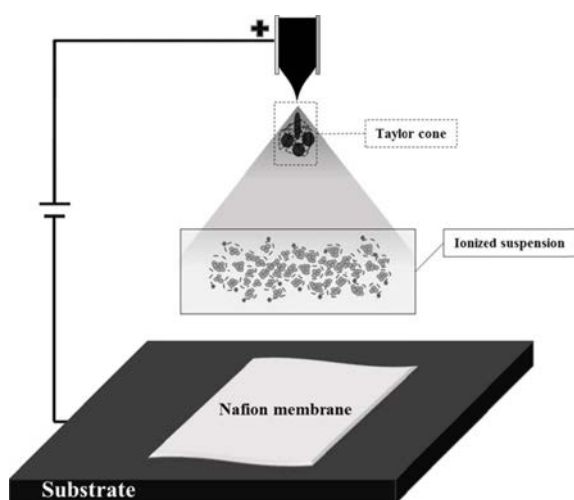


Fig. 1. Schematic illustration of the electro spraying process.

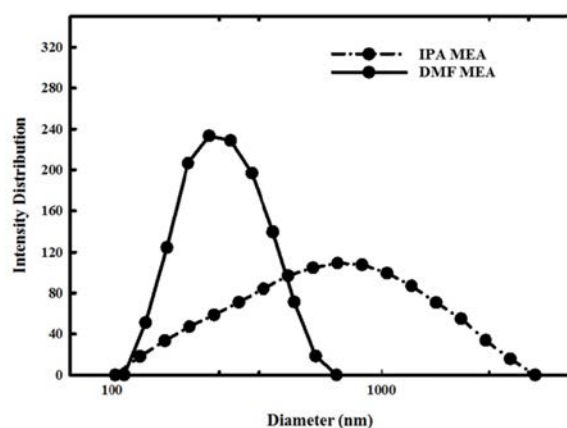


Fig. 2. Size distribution of Pt/C-Nafion agglomerates in catalyst ink measured by DLS.

with the solvent, evaporating along the float as well as after the deposition. Hence, it is essential to investigate how different solvents, i.e. IPA and DMF, affect the deposition process. IPA and DMF are two of the most widely used solvents in catalyst inks for PEMFC applications. Theoretically, IPA should evaporate easily in the electric field because it is quite volatile and its boiling point is as low as 82 °C. Accordingly, the droplets can reach the surfaces of the membrane with an insufficient amount of adsorbed solvent molecules, resulting in a severely agglomerated structure with large deviations in the catalyst layer thickness. Compared to IPA, a sufficient amount of DMF remained in the droplets along the float, due to the higher boiling point of DMF (> 153 °C). As a result, the more dense and compact catalyst layer structure was formed after use of the DMF instead of the IPA as the dispersing solvent.

In addition, the size of the Pt/C-Nafion agglomerates in the two catalyst inks is important in the fine electro-spray system. Fig. 2 shows the size distribution of Pt/C-Nafion agglomerates in the catalyst inks measured

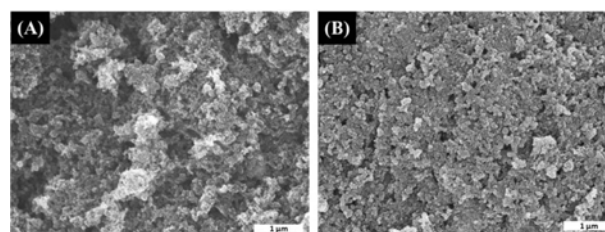


Fig. 3. SEM images of the catalyst layer surfaces of (A) the IPA and (B) DMF MEAs.

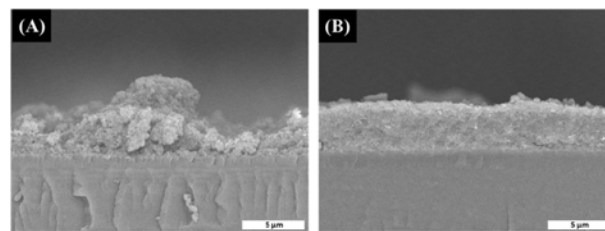


Fig. 4. SEM images of the cross section of (A) the IPA and (B) DMF MEAs.

using DLS analysis. There is a wide peak for the IPA solvent in the range of 100 nm–3600 nm, and the agglomerate sizes were inhomogeneous. However, in the DMF solvent catalyst ink, the diameter size was mostly in the range of 110 nm–680 nm, and the diameter corresponding to the peak was approximately 245 nm. This indicates that the DMF solvent disperses the catalyst better than the IPA solvent. Furthermore, the small size of the agglomerates passes the metal nozzle easily and subsequently maintains the cone-jet at the end of the metal nozzle.

Fig. 3 shows the SEM images on the surface of the catalyst layer fabricated with the two different solvents. As presented in Fig. 3(A), the catalyst layer had an inhomogeneous pore structure with the use of the IPA-based ink, in which the Pt/C catalyst and Nafion ionomer were agglomerated into large sphere-like structures with diameters ranging from 0.5 to 2 µm. This may be attributed to loss of the repulsive force resulting from the solvent dry out. In contrast, the catalyst layer fabricated with the DMF-based ink exhibited a more evenly distributed web-like structure, due to the residual DMF solvent in the surface of the electrode and the small size of the agglomerates inside the residual solvent. As a result, reactant gases such as H₂ and O₂ can penetrate deeper into the agglomerated catalyst layer, leading to better cell performance.

The cross-sectional SEM images of the catalyst layers fabricated with the IPA-based and DMF-based inks are presented in Fig. 4(A) and 4(B), respectively. While the average thickness of the two catalyst layers remained similar at approximately 3 to 6 µm, the DMF catalyst layer had a more uniformly distributed structure compared to the IPA catalyst layer. This is consistent with the SEM images of the surfaces of the two catalyst layers. Therefore, the number of charged

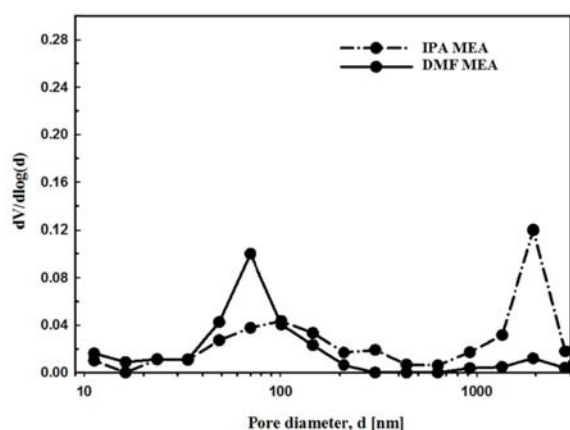


Fig. 5. Mercury porosimetry of the IPA and DMF MEAs catalyst layer.

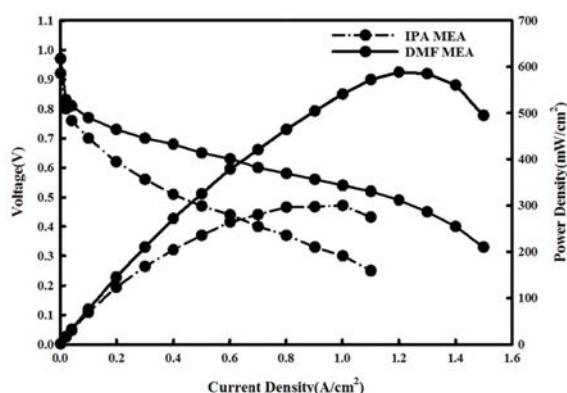


Fig. 6. Cell polarization curves of IPA and DMF MEAs.

species in the droplets, which is proportional to the solvent residuals, plays an important role in determining the morphology of the catalyst layer.

To further study the morphology of the catalyst layer, the pore size distributions of IPA MEAs and DMF MEAs are shown in Fig. 5. There are two part ranges for the IPA MEA catalyst layer below the pore diameter of 3000 nm. The smaller part is in the range of 30–200 nm; this range was attributed to the micropores inside the Pt/C-Nafion agglomerates. The large part, in the range of 1400–2800 nm, was mainly attributed to macro-pores, and the pore size was evenly distributed. However, in the DMF MEA catalyst layer, nearly all of the pores existed in the range of 30–200 nm relative to the IPA MEA catalyst layer, and the diameter corresponding to the peak was approximately 70 nm. This confirmed that using the DMF solvent resulted in a dense catalyst layer.

Single cell testing

Fig. 6 shows the cell polarization curves for the IPA and DMF MEAs with the same Pt loading of $0.05 \text{ mg}_{\text{Pt}}/\text{cm}^2$. All of the MEAs were prepared under the same experimental conditions. As observed in the figure, the performance of the DMF MEAs was superior to that of the IPA MEAs at all current density

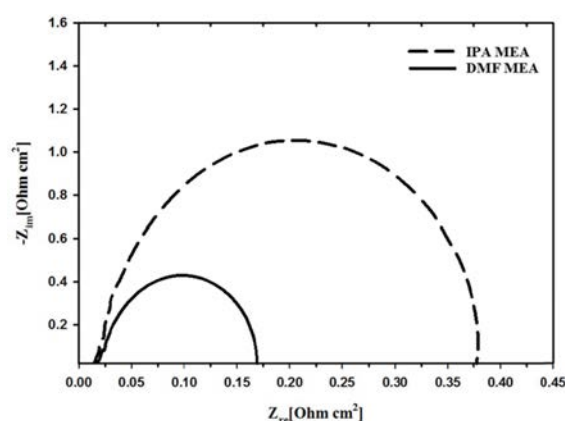


Fig. 7. Impedance spectra of the IPA and DMF MEAs at 0.80 V.

ranges. The current density for the DMF MEAs was 1.2 A cm^{-2} at the cell voltage of 0.5 V, which was 2.4 times higher than that of the IPA MEAs (0.5 A cm^{-2} at 0.5 V). In the intermediate- and high-current regions, the IPA MEAs showed both a slightly decreased performance and lower ohmic slope for the cell polarization. Maximum power densities of 600 mW cm^{-2} and 300 mW cm^{-2} were obtained for the DMF and IPA MEAs, respectively. This might be due to the dense and well-dispersed agglomerates, which reduced the charge and mass-transfer resistance.

Fig. 7 presents the impedance spectra for the DMF MEAs at 0.80 V as compared with the IPA MEAs. As seen in the figure, the high frequency resistance (HFR) of the IPA and DMF MEAs was approximately $0.015 \Omega \text{ cm}^2$. However, the charge-transfer resistance of the IPA MEAs was more than double that of the DMF MEAs, which could be explained by the fact that the DMF MEAs had better cell performance than the IPA MEAs.

Conclusions

In this work, we demonstrated that different solvents, specifically IPA and DMF, in catalyst ink affect the size of the agglomerates. The DMF solvent has a high boiling point ($> 153^\circ\text{C}$) and homogeneously disperses Nafion ionomers. To compare the agglomerated sizes in the IPA-based and DMF-based catalyst inks, DLS analysis was performed. The results of this analysis confirmed the narrow and even size distribution of the agglomerates in the DMF-based ink. The small size of the agglomerates coupled with the high boiling point resulted in a dense catalyst layer. To identify the dense structure, we measured the pore size distribution using mercury porosimetry; the DMF MEAs had smaller pore sizes ranging from 30 to 200 nm with a narrow distribution compared with the IPA MEAs. According to fuel cell performance test results, the cell performance of the DMF MEAs was approximately 2.4 times higher than

that of the IPA MEAs. As a result, the catalyst layer fabricated with DMF-based catalyst ink had a dense structure, and we concluded that control of the catalyst layer structure is an essential factor in increasing the cell performance.

Acknowledgements

This research was supported by the Korea Electrotechnology Research Institute (KERI) and the New & Renewable Energy Core Technology Program of the Korea Institute of Energy Technology Evaluation and Planning (KETEP).

References

1. H.P. Dhar, *J. Electroanalytical Chemistry* 357 (1993) 237-250.
2. W. Sun, A.B. Peppley, and K. Karan, *Electrochim. Acta* 50[16] (2005) 3359-3374.
3. B. Millington, V. Whipple, and B.G. Pollet, *J. Power Sources* 196 (2011) 8500-8508.
4. C.Y. Liu, and C.C. Sung, *J. Power Sources* 220 (2012) 348-353.
5. M.S. Saha, D.K. Paul, D. Malevich, B.A. Peppley, and K. Karan, *ECS transactions* 25[1] (2009) 2049-2059.
6. R. Benitez, J. Soler and L. Daza, *J. Power Sources* 151[10] (2005) 108-113.
7. R. Benitez, A.M. Chaparro and L. Daza, *J. Power Sources* 151[10] (2005) 2-10.
8. A.M. Chaparro, R. Benitez, L. Gubler, G.G. Scherer and L. Daza, *J. Power Sources* 169[1] (2007) 77-84.
9. A.M. Chaparro, B. Gallardo, M.A. Folgado, A.J. Martina and L. Daza, *Catalysis Today*, 143 (2009) 237-241.
10. S. Martin, P.L. Garcia-Ybarra and J.L. Castillo, *J. Power Sources* 195[9] (2010), 2443-2449.
11. S. Martin, P.L. Garcia-Ybarra and J.L. Castillo, *Int. J. Hydrogen Energy* 35[19] (2010) 10446-10451.
12. A.M. Chaparro, M.A. Folgado, P. Ferreira-Aparicio, A.J. Martín, I. Alonso-Alvarez and L. Daza, *J. Electrochem. Soc.* 157[7] (2010) B993-B999.
13. A.M. Chaparro, P. Ferreira-Aparicio, M.A. Folgado, A.J. Martina and L. Daza, *J. Power Sources* 196[9] (2011) 4200-4208.
14. S. Martin, B. Martinez-Vazquez, P.L. Garcia-Ybarra and J.L. Castillo, *J. Power Sources* 229[1] (2013) 179-184.
15. M.A. Folgado, P. Ferreira-Aparicio and A.M. Chaparro, *Int. J. Hydrogen Energy* 41[1] (2016) 505-515.
16. A.M. Chaparro, P. Ferreira-Aparicio, M.A. Folgado, E. Brightman, G. Hinds, *J. Power Sources* 325[1] (2016) 609-619.
17. S. Wang, G. Sun, Z. Wu, and Q. Xin, *J. Power Sources* 165 (2007) 128-133.
18. S.H. Park, H.N. Yang, D.C. Lee, K.W. Park, W.J. Kim, *Electrochim. Acta* 125 (2014) 141-148.
19. C.Y. Jung, T.H. Kim and S.C. Yi, *Chem. Sus. Chem.* 7[2] (2014) 466-473.